^{89}Zr as a PET Surrogate Radioisotope for Scouting Biodistribution of the Therapeutic Radiometals ^{90}Y and ^{177}Lu in Tumor-Bearing Nude Mice After Coupling to the Internalizing Antibody Cetuximab

Lars R. Perk, MSc[1]; Gerard W.M. Visser, PhD[2]; Maria J.W.D. Vosjan, BSc[1]; Marijke Stigter-van Walsum, BSc[1]; Bernard M. Tijink, MD[1]; C. René Leemans, MD, PhD[1]; and Guus A.M.S. van Dongen, PhD[1]

[1]Department of Otolaryngology/Head and Neck Surgery, VU University Medical Center, Amsterdam, The Netherlands; and [2]Department of Nuclear Medicine and PET Research, VU University Medical Center, Amsterdam, The Netherlands

Immuno-PET as a scouting procedure before radioimmunotherapy (RIT) aims at confirming tumor targeting and accurately estimating radiation dose delivery to both tumor and normal tissues and might therefore be of value for selection of patient candidates for RIT. A prerequisite for this approach is that PET radioimmunoconjugates and RIT radioimmunoconjugates must show a similar biodistribution. In the present study, we evaluated the potential of the long-lived positron emitter ^{89}Zr to predict biodistribution of the residualizing therapeutic radiometals ^{88}Y (as a substitute for ^{90}Y) and ^{177}Lu when labeled to the monoclonal antibody (mAb) cetuximab via different types of chelates. Cetuximab was selected as a model mAb because it abundantly internalizes after binding to the epidermal growth factor receptor. **Methods:** Cetuximab was labeled with ^{89}Zr using succinylated desferrioxamine B (*N*-sucDf). The chelates *p*-benzyl isothiocyanate-1,4,7,10-tetraazacyclododecane-1,4,7,10-tetraacetic acid (*p*-SCN-Bz-DOTA) and *p*-isothiocyanatobenzyl diethylenetriaminepentaacetic acid (*p*-SCN-Bz-DTPA) were both used for radiolabeling with ^{88}Y and ^{177}Lu. For measurement of the in vitro stability of each of the 5 radioimmunoconjugates, samples were incubated in freshly prepared human serum at 37°C up to 16 d. Biodistribution was assessed at 24, 48, 72, and 144 h after intraperitoneal coinjection of the PET and RIT conjugates in nude mice bearing the squamous cell carcinoma xenograft line A431. **Results:** Cetuximab premodification with *N*-sucDf, *p*-SCN-Bz-DOTA, or *p*-SCN-Bz-DTPA resulted in chelate-to-mAb molar ratios of about 1. After radiolabeling and purification, the radiochemical purity and immunoreactive fraction of the conjugates always exceeded 97% and 93%, respectively. All conjugates were stable in serum, showing a radioactivity release of less than 5% until day 7. From day 7 until day 16, an enhanced release was observed for the ^{89}Zr-*N*-sucDf, ^{88}Y-*p*-SCN-Bz-DTPA, and ^{177}Lu-*p*-SCN-Bz-DTPA conjugates. The coinjected PET and RIT conjugates showed similar biodistributions, except for the thighbone and sternum. For example, the ^{89}Zr-*N*-sucDf conjugate showed a 2.0–2.5 times higher radioactivity accretion in the thighbone than did the RIT conjugates at 72 h after injection. **Conclusion:** In view of the advantages of PET over SPECT, ^{89}Zr-immuno-PET is a promising modality for in vivo scouting of ^{90}Y- and ^{177}Lu-labeled mAbs, although care should be taken when estimating bone marrow doses.

Key Words: ^{89}Zr; immuno-PET; ^{90}Y; ^{177}Lu; radioimmunotherapy

J Nucl Med 2005; 46:1898–1906

Tumor targeting using radiolabeled monoclonal antibodies (mAbs) in radioimmunotherapy (RIT) is developing into an attractive approach to cancer treatment. In the past few years, the U.S. Food and Drug Administration has approved 2 RIT pharmaceuticals for the treatment of non-Hodgkin's lymphoma: the anti-CD20 mAbs ^{90}Y-ibritumomab tiuxetan (Zevalin; IDEC and Schering) and ^{131}I-tositumomab (Bexxar; Corixa and GlaxoSmithKline). Several new radioimmunoconjugates are currently being evaluated in clinical trials (*1*). Besides ^{90}Y and ^{131}I, also ^{177}Lu is a commonly used β-emitter in these RIT trials. ^{90}Y and ^{177}Lu are residualizing radiometals that show higher retention in tumors than do the nonresidualizing labels ^{131}I and ^{186}Re and therefore are especially attractive in combination with internalizing mAbs (*2–4*). The β^- energy of ^{177}Lu and the related maximal particle range of 1.5 mm make this radionuclide particularly well suited for eradication of minimal residual disease, whereas ^{90}Y is the radionuclide of choice for treatment of bulky tumors because of its higher β^- energy and related maximal particle range of 12.0 mm (*5*). The most effective approach when tumors of various sizes have to be treated might even be combination of both radionuclides in a single therapy (*6*).

Received Jun. 23, 2005; revision accepted Aug. 4, 2005.

For correspondence or reprints contact: Guus A.M.S. van Dongen, PhD, Department of Otolaryngology/Head and Neck Surgery, VU University Medical Center, De Boelelaan 1117, P.O. Box 7057, 1007 MB Amsterdam, The Netherlands.

E-mail: gams.vandongen@vumc.nl

Both the ^{90}Y-ibritumomab tiuxetan and the ^{131}I-tositumomab treatment regimens are preceded by a γ-camera imaging procedure for selection of patient candidates for RIT (*7,8*). Performing radioimmunoscintigraphy with trace-labeled mAbs as a scouting procedure before RIT aims at confirming tumor targeting and quantifying biodistribution to allow estimation of dose delivery to tumors and normal tissues (*9*). Alternatively, this approach can also be used for in vivo characterization of new mAb candidates for use in RIT. For pretherapy imaging in such a setting, γ-emitters are coupled to mAbs, whereas optimal prediction is obtained only when imaging and therapeutic radioimmunoconjugates show similar biodistributions. ^{177}Lu emits a small proportion of γ-radiation (208 keV, 11%) but until now has not been used at a trace dose for clinical scouting. ^{90}Y is a pure β-emitter, and therefore ^{111}In is often used as a γ-emitting surrogate for tracing the biodistribution of the ^{90}Y-labeled mAbs. For coupling of ^{177}Lu, ^{90}Y, and ^{111}In to mAbs, DOTA and DTPA chelates are mostly used. Although DOTA gives the most stable complexes, DTPA is the chelate of choice for obtaining reliable high labeling yields and conjugates with high specific activities (*2,10*). Unfortunately, the current use of γ-camera imaging for quantification of ^{111}In/^{177}Lu-labeled mAbs has intrinsic limitations, primarily on account of scatter and partial absorption of γ-photons in the patient. Besides this, differences in biodistribution between ^{111}In-mAb and ^{90}Y-mAb conjugates have been observed in vivo in tumor-bearing mice and in cancer patients (*11–13*).

Recently, we introduced the long-lived positron emitter ^{89}Zr (half-life, 78.4 h) as a promising residualizing radionuclide for PET of mAbs (^{89}Zr-immuno-PET). PET is better qualified for tracer quantification because of more accurate scatter and attenuation correction and superior spatial and temporal resolution for imaging. ^{89}Zr was coupled to mAbs—the chimeric mAb U36 among them—via the chelate *N*-succinyldesferrioxamine B (*N*-sucDf). We demonstrated that quantitative PET with ^{89}Zr was feasible (*14*). Moreover, in preliminary studies the chimeric mAb U36-*N*-sucDf-^{89}Zr showed a biodistribution similar to that of the chimeric mAb U36-*p*-SCN-Bz-DOTA-^{88}Y (with ^{88}Y as a γ-emitting substitute for ^{90}Y) in nude mice bearing the head and neck cancer xenograft line HNX-OE (*14*). This model, however, was not representative of more extensively internalizing antibodies.

In the present study, we extended the scope of ^{89}Zr-immuno-PET by using cetuximab (Erbitux; ImClone Systems) as an abundantly internalizing model mAb and nude mice bearing the squamous cell carcinoma xenograft line A431 as the tumor model (*15*). Cetuximab is a chimeric IgG1 mAb that binds with high affinity to the epidermal growth factor receptor (EGFR) (*16*). The cell line A431 shows abundant expression of EGFR (*17*). The potential of ^{89}Zr to predict the biodistribution of the residualizing labels ^{177}Lu and ^{90}Y was evaluated in a comprehensive way by coinjection of conjugates. To this end, cetuximab-*N*-sucDf-^{89}Zr was administered with cetuximab-*p*-SCN-Bz-DOTA-^{88}Y, cetuximab-*p*-SCN-Bz-DOTA-^{177}Lu, cetuximab-*p*-SCN-Bz-DTPA-^{88}Y, or cetuximab-*p*-SCN-Bz-DTPA-^{177}Lu, and biodistribution in mice was assessed up to 6 d after injection. Before these biodistribution studies, the in vitro stability of the conjugates in human plasma was analyzed.

MATERIALS AND METHODS

mAb, Cell Line, and Radioactivity

The mAb cetuximab was purchased from ImClone Systems. Cetuximab is a chimeric IgG1 mAb that binds with high affinity to the EGFR, blocks ligand-induced activation of the receptor tyrosine kinase, and induces dimerization and downregulation of the EGFR, which prevents further binding and activation by the ligands (*16*). The human squamous cell carcinoma cell line A431, carrying an amplification of the EGFR gene, was obtained from the American Type Culture Collection (ATCC number CRL-1555).

^{89}Zr (2.7 GBq/mL in 1 mol of oxalic acid per liter) was produced by Cyclotron BV by a (p,n) reaction on natural ^{89}Y and purified with a hydroxamate column (*18*). ^{88}Y (37 MBq/mL in 0.1 mol of HCl per liter) was obtained from Isotope Products Europe, ^{177}Lu (9.25 GBq/mL in 0.05 mol of HCl per liter) from Perkin-Elmer, ^{111}In (370 MBq/mL in 0.05 mol of HCl per liter) from Tyco Healthcare, and ^{125}I (3.7 GBq/mL in 0.01 mol of NaOH per liter) from Amersham.

Radiolabeling

For ^{89}Zr, ^{88}Y, and ^{177}Lu labeling of mAbs, modification procedures were established to arrive at a chelate-to-mAb molar ratio of 1:1.

Preparation of ^{89}Zr-Labeled Cetuximab. mAb labeling with ^{89}Zr was achieved starting with the chelate desferrioxamine B (Df) (Desferal; Novartis) as described previously (*17*). In short, Df was succinylated (*N*-sucDf), temporarily filled with iron (Fe(III)), and coupled to cetuximab by means of a tetrafluorophenol-*N*-sucDf ester. After removal of Fe(III) by transchelation to ethylenediaminetetraacetic acid (EDTA), the premodified mAb was purified on a PD10 column (eluent: 0.9% NaCl/gentisic acid, 5 mg/mL; pH 5.0). Subsequently, *N*-sucDf-cetuximab was labeled with ^{89}Zr in *N*-2-hydroxyethylpiperazine-*N*-2-ethanesulfonic acid (HEPES) buffer at pH 7.0. Finally, ^{89}Zr-*N*-sucDf-cetuximab was purified on a PD10 column (eluent: 0.9% NaCl/gentisic acid, 5 mg/mL; pH 5.0) to remove any unbound ^{89}Zr.

Preparation of ^{88}Y- or ^{177}Lu-Labeled Cetuximab. Cetuximab was conjugated with *p*-benzyl isothiocyanate-1,4,7,10-tetraazacyclododecane-1,4,7,10-tetraacetic acid (*p*-SCN-Bz-DOTA) or *p*-isothiocyanatobenzyl diethylenetriaminepentaacetic acid (*p*-SCN-Bz-DTPA) (Macrocyclics). All steps were performed under strict metal-free conditions. Before use, cetuximab was extensively dialyzed (Slide-A-Lyzer dialysis cassettes; Pierce Biotechnology) against metal-free $NaHCO_3$ (0.1 mol/L, pH 9.0) containing 2 g of Chelex 100 (Bio-Rad) per liter. For conjugation, 125 μL of *p*-SCN-Bz-DOTA or *p*-SCN-Bz-DTPA (1.6 mg/mL in $NaHCO_3$, 0.1 mol/L; pH 9.0), 175 μL of $NaHCO_3$ (0.1 mol/L, pH 9.0), and 700 μL of dialyzed cetuximab (1.4 mg) were incubated for 30 min at 37°C. The modified cetuximab was purified using a prewashed PD-10 column and eluted with CH_3COONH_4 (0.25 mol/L, pH 5.5). The cetuximab-*p*-SCN-Bz-DOTA and cetuximab-*p*-SCN-Bz-DTPA conjugates (~0.5 mg) were labeled with either ^{88}Y (1.5 MBq) or ^{177}Lu (28 MBq) in CH_3COONH_4 (0.25 mol/L, pH 5.5) for

60 min at 45°C (*p*-SCN-Bz-DOTA conjugates) or at room temperature (*p*-SCN-Bz-DTPA conjugates), in a total reaction volume of 1 mL. After labeling, 50 μL of EDTA, 0.05 mol/L, were added to the reaction vial, and the mixture was incubated for another 5 min. Nonconjugated ^{88}Y or ^{177}Lu was removed using a PD-10 column with 0.9% NaCl as eluent. The first 2.5 mL (1.0-mL sample volume and the first 1.5 mL) were discarded, and the radiolabeled cetuximab was collected in the next 1.5 mL.

Preparation of ^{125}I-Labeled Cetuximab. Iodination of cetuximab with ^{125}I was performed essentially as described previously (*19*). In short, 20-mL β-scintillation glass vials were coated with 75 μg of IODO-GEN (Pierce Biotechnology) in CH_2Cl_2 and dried under a stream of N_2 gas, resulting in a thin coating of IODO-GEN on the bottom surface of the vial. The vials were stored under N_2 atmosphere. To an IODO-GEN–coated glass vial, 50 μL of Na_2HPO_4 (0.5 mol/L, pH 7.4), 194 μL of Na_2HPO_4 (0.1 mol/L, pH 6.8), 250 μL of cetuximab (2 mg/mL), and 55 MBq of ^{125}I in 6.4 μL of NaOH (1 mmol/L) were successively added. After gentle shaking for 4 min at room temperature, 0.1 mL of ascorbic acid (25 mg/mL, pH 5) was added. After an additional 5 min, the reaction mixture was transferred to a syringe connected to a filter (0.2-μm Acrodisc; Gelman Sciences) followed by 0.4 mL of Na_2HPO_4 (0.1 mol/L, pH 6.8), used for an additional rinsing of the reaction vial. This combined solution was filtered and then purified on a PD-10 column with 0.9% NaCl/ascorbic acid (5 mg/mL, pH 5) as eluent. The first 2.5 mL (1.0-mL sample volume and the first 1.5 mL) were discarded, and the radioiodinated cetuximab was collected in the next 1.5 mL.

Analyses

All conjugates were analyzed by instant thin-layer chromatography (ITLC) for radiochemical purity, by high-performance liquid chromatography and sodium dodecylsulfate-polyacrylamide gel electrophoresis followed by phosphor imager analyses for integrity, and by a cell-binding assay for immunoreactivity. ITLC analysis of radiolabeled cetuximab was performed on silica gel–impregnated glass fiber sheets (Gelman Sciences). As the mobile phase, citrate buffer (20 mmol/L, pH 5.0) was used for ^{125}I- and ^{89}Zr-labeled mAbs. ITLC samples of ^{88}Y- and ^{177}Lu-labeled mAbs were first incubated for 5 min in an EDTA solution (20 mmol/L) and subsequently spotted on ITLC. As the mobile phase, 0.9% NaCl was used. The radioimmunoconjugates were monitored by high-performance liquid chromatography as described previously (*18*). Gel electrophoresis was performed on a Pharmacia Phastgel System (Amersham Biosciences) using 7.5% sodium dodecylsulfate–polyacrylamide gel electrophoresis gels (Amersham Biosciences) under nonreducing conditions and analyzed on a phosphor imager. In vitro binding characteristics of radiolabeled cetuximab were determined in an immunoreactivity assay essentially as described by Lindmo et al. (*20*), using A431 cells fixed with 2.0% paraformaldehyde.

Determination of Chelate-to-mAb Ratio

The Desferal-to-cetuximab molar ratio was determined by high-performance liquid chromatography analysis using ^{59}Fe as described by Verel et al. (*18*). *p*-SCN-Bz-DOTA-to-mAb and *p*-SCN-Bz-DTPA-to-mAb molar ratios were determined following a method described by Meares et al. (*21*). In short, conjugates were labeled according to the aforementioned procedures, with a known excess of indium acetate spiked with ^{111}In. After labeling, the solution was challenged with EDTA and subsequently spotted on ITLC. Antibody-bound ^{111}In remained at the origin, whereas unreacted ^{111}In (as ^{111}In-EDTA) moved with R_f 0.8–1.0. ITLC data were used to calculate the chelate-to-mAb molar ratio. For double-checking of *p*-SCN-Bz-DOTA-to-mAb and *p*-SCN-Bz-DTPA-to-mAb molar ratios, the same procedure was performed using an excess of lutetium acetate spiked with ^{177}Lu.

Serum Stability

For measurement of the in vitro stability of each of the individual radioimmunoconjugates, samples containing 100 μg of mAb were incubated in freshly prepared human serum (1:1 v/v dilution; total volume, 1 mL) at 37°C in a humidified incubator maintained at 5% CO_2 and 95% air. At various intervals (1, 3, 5, 7, 9, 13, and 16 d), aliquots were taken and analyzed by ITLC and high-performance liquid chromatography.

Biodistribution Study

Nude mice bearing subcutaneously implanted xenografts of the human tumor line A431 were used. The female mice we used for this experiment (athymic *nu/nu*, 21–31 g; Harlan CPB) were 8–10 wk old at the time of the experiment. All animal experiments were performed according to National Institutes of Health principles of laboratory animal care and Dutch national law ("Wet op de dierproeven", Stb 1985, 336).

In 4 experiments (Table 1), 64 mice were simultaneously injected intraperitoneally with ^{89}Zr-labeled cetuximab combined with either ^{88}Y- or ^{177}Lu-labeled cetuximab. In all animals, unlabeled cetuximab was added to the injection up to a total of 500 μg. At 24, 48, 72, and 144 h after injection, 4 mice per group and time

TABLE 1
Radioimmunoconjugates Used for the Biodistribution Study

Experiment	Radioimmunoconjugate	Activity per mouse (kBq)	Radiochemical purity (%)	Immunoreactivity (%)
1	Cetuximab-*p*-SCN-Bz-DOTA-^{88}Y	60	99.2	94
	Cetuximab-*N*-sucDf-^{89}Zr	500	98.0	93
2	Cetuximab-*p*-SCN-Bz-DOTA-^{177}Lu	370	98.8	97
	Cetuximab-*N*-sucDf-^{89}Zr	500	98.0	93
3	Cetuximab-*p*-SCN-Bz-DTPA-^{88}Y	47	98.0	97
	Cetuximab-*N*-sucDf-^{89}Zr	320	97.8	97
4	Cetuximab-*p*-SCN-Bz-DTPA-^{177}Lu	170	99.4	96
	Cetuximab-*N*-sucDf-^{89}Zr	320	97.8	97
5	Cetuximab-*p*-SCN-Bz-DOTA-^{177}Lu	370	99.0	96
	Cetuximab-^{125}I	370	99.8	98

point were anesthetized, bled, killed, and dissected. Blood, tumor, skin, sternum, heart, lung, liver, spleen, kidney, muscle, thighbone, colon, ileum, and stomach were weighed, and the amount of radioactivity in each tissue was assessed in a γ-well counter (Wallac LKB-CompuGamma 1282; Pharmacia). The 511-keV γ-energy of ^{89}Zr and the 1,837-keV γ-energy of ^{88}Y were used for dual-isotope counting of the coinjected ^{88}Y/^{89}Zr-labeled mAbs, and the 909-keV γ-energy of ^{89}Zr and the 208-keV γ-energy of ^{177}Lu were used for dual-isotope counting of the coinjected ^{177}Lu/^{89}Zr-labeled mAbs. Crossover corrections from one radionuclide into the alternate window were performed using a standard of each radionuclide. To correct for radioactive decay, injection standards were counted simultaneously.

In a fifth experiment (Table 1), 14 mice were injected intraperitoneally with cetuximab-^{125}I combined with cetuximab-*p*-SCN-Bz-DOTA-^{177}Lu, and unlabeled cetuximab was added to the injection up to a total of 1 mg. At 24 h (n = 3), 48 h (n = 4), 72 h (n = 3), and 120 h (n = 4) after injection, the mice were anesthetized, bled, killed, and dissected, with further processing according to the above procedure.

Radioactivity uptake was calculated as the percentage of the injected dose per gram of tissue (%ID/g). Differences in tissue uptake between coinjected conjugates were statistically analyzed for each time point with SPSS 11.0 (SPSS Inc.) using the Student t test for paired data. Two-sided significance levels were calculated, and $P < 0.05$ was considered statistically significant. Statistical analysis of differences in thighbone uptake between groups was performed using 1-way ANOVA.

RESULTS

Conjugation and Radiolabeling

Within the applied stoichiometry, premodification of cetuximab resulted in 0.8–1.2 *N*-sucDf, *p*-SCN-Bz-DOTA, or *p*-SCN-Bz-DTPA moieties per mAb. Subsequent labeling of cetuximab-*N*-sucDf with ^{89}Zr and cetuximab-*p*-SCN-Bz-DOTA or cetuximab-*p*-SCN-Bz-DTPA with ^{88}Y or ^{177}Lu resulted in overall labeling yields of >70%. The radiochemical purity was at least 97% for all 5 products (Table 1). Labeling of cetuximab with ^{125}I resulted in an overall labeling yield of 89%, and the radiochemical purity was 99.8% for the purified product. Immunoreactivity for all cetuximab conjugates was more than 93% at the highest cell concentration. The specific activities for the biodistribution studies were 78 MBq/mg for cetuximab-*N*-sucDf-^{89}Zr, 0.49 MBq/mg for cetuximab-*p*-SCN-Bz-DOTA-^{88}Y, 37 MBq/mg for cetuximab-*p*-SCN-Bz-DOTA-^{177}Lu, 0.41 MBq/mg for cetuximab-*p*-SCN-Bz-DTPA-^{88}Y, 26 MBq/mg for cetuximab-*p*-SCN-Bz-DTPA-^{177}Lu, and 109 MBq/mg for cetuximab-^{125}I.

In Vitro Stability

All conjugates were individually tested for stability in human serum. These results are shown in Table 2. Cetuximab-*N*-sucDf-^{89}Zr, cetuximab-*p*-SCN-Bz-DOTA-^{88}Y, and cetuximab-*p*-SCN-Bz-DOTA-^{177}Lu were stable until day 7; <3% of the radiolabel was released during this incubation period. Cetuximab-*p*-SCN-Bz-DTPA-^{88}Y and cetuximab-*p*-SCN-Bz-DTPA-^{177}Lu showed a slightly faster radiometal release during this period (4.6% and 4.3%, respectively). After day 7, the latter conjugates and also cetuximab-*N*-sucDf-^{89}Zr showed an accelerated release of radiolabel when compared with cetuximab-*p*-SCN-Bz-DOTA-^{88}Y and cetuximab-*p*-SCN-Bz-DOTA-^{177}Lu. At day 16, there was a total release of 22.4%, 23.5%, and 17.4% for cetuximab-*p*-SCN-Bz-DTPA-^{88}Y, cetuximab-*p*-SCN-Bz-DTPA-^{177}Lu, and cetuximab-*N*-sucDf-^{89}Zr, respectively, versus 4.0% and 2.9% for cetuximab-*p*-SCN-Bz-DOTA-^{88}Y and cetuximab-*p*-SCN-Bz-DOTA-^{177}Lu, respectively.

Biodistribution Study

For comparison of the biodistribution of ^{89}Zr-labeled mAb with ^{88}Y- or ^{177}Lu-labeled mAb, cetuximab-*N*-sucDf-^{89}Zr was coinjected in tumor-bearing mice with cetuximab-*p*-SCN-Bz-DOTA-^{88}Y (experiment 1), cetuximab-*p*-SCN-Bz-DOTA-^{177}Lu (experiment 2), cetuximab-*p*-SCN-Bz-DTPA-^{88}Y (experiment 3), or cetuximab-*p*-SCN-Bz-DTPA-^{177}Lu (experiment 4). The essential characteristics of the radiolabeled immunoconjugates used in the biodistribution study are shown in Table 1, and the corresponding biodistributions are summarized in Figures 1-4. At the time of dissection, the tumor weights (mean ± SD) were 61 ± 72, 78 ± 65, 189 ± 176, and 148 ± 110 mg for experiments 1, 2, 3, and 4, respectively. The radioactivity uptake in tumor and most other tissues was comparable between ^{89}Zr-labeled cetuximab on the one hand and ^{88}Y- or ^{177}Lu-labeled cetuximab on the other hand (Figs. 1–4). The only consistent difference observed was a significantly higher uptake for ^{89}Zr than for ^{88}Y and ^{177}Lu in thighbone and sternum at all time points except 24 h after injection in thighbone for experiment 1 (Fig. 1, P = 0.176) and experiment 3 (Fig. 3, P = 0.096). At 72 h after injection, the mean thighbone uptake

TABLE 2
In Vitro Stability of Radioimmunoconjugates upon Incubation at 37°C in Human Serum

Conjugate	Radiochemical purity (%)							
	0 d	1 d	3 d	5 d	7 d	9 d	13 d	16 d
^{89}Zr-*N*-sucDf-mAb	97.5	98.0	97.0	96.7	95.3	94.4	88.9	80.1
^{88}Y-*p*-SCN-Bz-DOTA-mAb	99.6	97.1	96.7	96.8	96.7	96.8	96.8	95.6
^{177}Lu-*p*-SCN-Bz-DOTA-mAb	99.7	98.5	97.6	98.7	98.6	97.9	97.5	96.8
^{88}Y-*p*-SCN-Bz-DTPA-mAb	97.5	98.4	95.2	93.8	92.9	89.7	81.9	75.1
^{177}Lu-*p*-SCN-Bz-DTPA-mAb	97.2	94.7	93.9	94.5	92.9	90.6	86.3	73.7

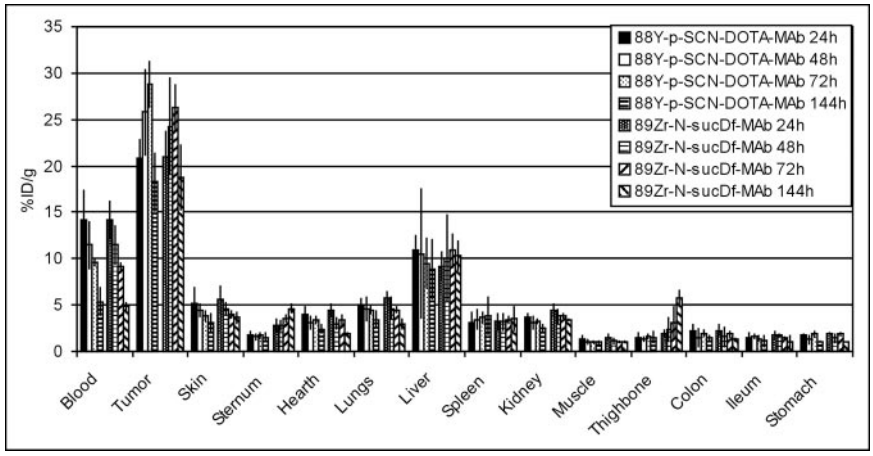

FIGURE 1. Biodistributions of intraperitoneally coinjected cetuximab-*N*-sucDf-^{89}Zr and cetuximab-*p*-SCN-Bz-DOTA-^{88}Y (experiment 1, total of 500 μg mAb) in A431 xenograft-bearing nude mice at 24, 48, 72, and 144 h after injection.

was between 3.2 and 4.7 %ID/g for ^{89}Zr, compared with 1.6 and 1.3 %ID/g for ^{88}Y- and ^{177}Lu-*p*-SCN-Bz-DOTA, respectively, and 2.3 and 2.0 %ID/g for ^{88}Y- and ^{177}Lu-*p*-SCN-Bz-DTPA, respectively. These data revealed that radioactivity accretion in thighbone was 2.0, 2.5, 2.0, and 2.4 times higher for the *N*-sucDf-^{89}Zr conjugates than for the *p*-SCN-Bz-DOTA-^{88}Y, *p*-SCN-Bz-DOTA-^{177}Lu, *p*-SCN-Bz-DTPA-^{88}Y, and *p*-SCN-Bz-DTPA-^{177}Lu conjugates, respectively. At 144 h, differences in thighbone were larger, with a mean uptake of between 4.8 and 6.9 %ID/g for ^{89}Zr, compared with 1.5 and 1.0 %ID/g for ^{88}Y- and ^{177}Lu-*p*-SCN-Bz-DOTA, respectively, and 2.4 and 2.0 %ID/g for ^{88}Y- and ^{177}Lu-*p*-SCN-Bz-DTPA, respectively.

An ANOVA showed that the thighbone uptake for both ^{177}Lu and ^{88}Y was significantly higher ($P < 0.05$) for the *p*-SCN-Bz-DTPA conjugates than for the *p*-SCN-Bz-DOTA conjugates at 72 h and 144 h. An exceptional observation was seen in mice coinjected with cetuximab-*N*-sucDf-^{89}Zr and cetuximab-*p*-SCN-Bz-DTPA-^{88}Y at 144 h after injection (Fig. 3). For both conjugates, we observed a much higher accumulation of activity in the liver and a concomitant enhanced drop in blood and tumor uptake when compared with the other experiments.

To illustrate the effect of abundant conjugate internalization and radionuclide residualization on radioactivity distribution, the biodistribution of coinjected ^{177}Lu-*p*-SCN-Bz-DOTA-cetuximab and ^{125}I-cetuximab was compared in the same animal model (experiment 5; Fig. 5). At the time of dissection, the tumor weight was 132 ± 72 mg (mean ± SD). The radioactivity uptake in tumor differed markedly; for example, at 72 h after injection, the mean tumor uptake was 21.9 %ID/g for the residualizing radionuclide ^{177}Lu, compared with 4.5 %ID/g for the nonresidualizing radionuclide ^{125}I. Also, radioactivity uptake levels in liver and, to a lesser degree, spleen, kidney, and skin differed substantially, with a higher uptake for ^{177}Lu than for ^{125}I. Blood values and values in all other organs were similar. For ^{125}I-cetuximab, the tumor-to-blood ratio never exceeded 1, notwithstanding the fact that ^{125}I-cetuximab was of the highest quality with respect to integrity and immunoreactivity.

DISCUSSION

Biodistribution may be accurately predicted—and delivery of radiation dose to tumors and critical organs estimated—by performing an immuno-PET scouting procedure before RIT. A prerequisite for this approach is that the PET and RIT conjugates of the mAb of interest must provide similar radioactivity biodistributions. Differences in radio-

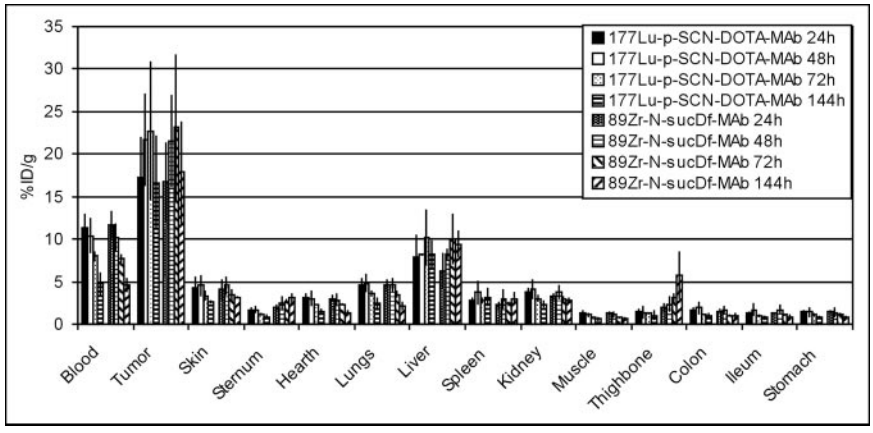

FIGURE 2. Biodistributions of intraperitoneally coinjected cetuximab-*N*-sucDf-^{89}Zr and cetuximab-*p*-SCN-Bz-DOTA-^{177}Lu (experiment 2, total of 500 μg mAb) in A431 xenograft-bearing nude mice at 24, 48, 72, and 144 h after injection.

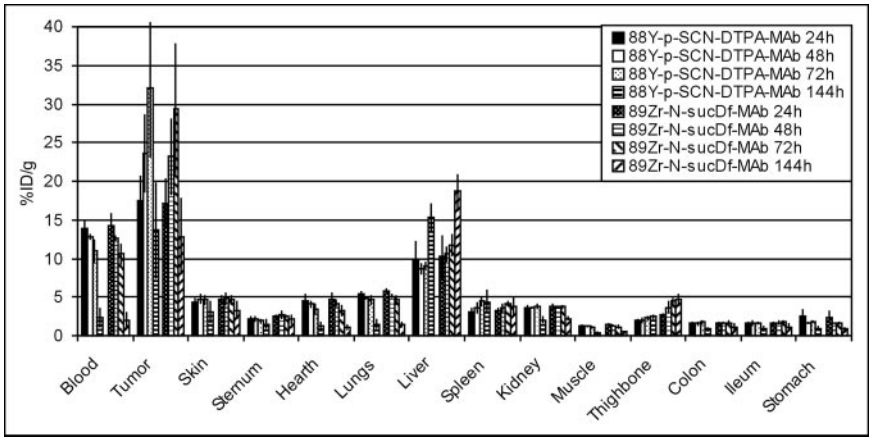

FIGURE 3. Biodistributions of intraperitoneally coinjected cetuximab-*N*-sucDf-^{89}Zr and cetuximab-*p*-SCN-Bz-DTPA-^{88}Y (experiment 3, total of 500 μg mAb) in A431 xenograft-bearing nude mice at 24, 48, 72, and 144 h after injection.

nuclide distribution might occur in several instances: when the mAb conjugates show altered and deviating pharmacokinetics (e.g., as a result of radiolabeling), when the radionuclide–chelate complexes exhibit different in vivo stabilities, when the radionuclides show deviating redistributions after release from the conjugate or catabolism (e.g., after internalization of the radioimmunoconjugate by the tumor cell), or when combinations of these and possibly other factors occur.

Recently, Verel et al. reported that the chimeric mAb U36-*N*-sucDf labeled with the positron emitter ^{89}Zr was able to monitor the biodistribution of the chimeric mAb U36-*p*-SCN-DOTA-^{88}Y in nude mice bearing HNSCC xenografts and that quantitative PET with ^{89}Zr is feasible (*14*). The conclusion from these studies was that ^{89}Zr and ^{90}Y form a perfect PET/RIT isotope pair. However, because only a minor proportion of chimeric mAb U36 internalizes after binding to its target antigen CD44v6, it might be that this does not hold true for abundantly internalizing mAbs.

Studies were therefore extended to assess the full potential of ^{89}Zr for predicting the biodistribution of residualizing therapeutic radiometals. First, the anti-EGFR mAb cetuximab was used for in vivo targeting of the xenograft line A431, because of the high rate of internalization (as illustrated by using a residualizing and a nonresidualizing radiolabel; Fig. 5). Second, the residualizing RIT radionuclide ^{88}Y (as a substitute for ^{90}Y) was tested along with ^{177}Lu. Finally, the chelate *p*-SCN-Bz-DOTA used for coupling of ^{90}Y and ^{177}Lu was tested along with *p*-SCN-Bz-DTPA. Although the pathlength and energy of its β^- particles make ^{90}Y the most suitable for RIT of large tumors, ^{177}Lu is the more favorable radionuclide for treatment of small tumors. Although complexes of these RIT radionuclides with DOTA are considered to be more stable than complexes with DTPA-like molecules (*22*), DTPA-like molecules are sometimes preferred because of the better labeling efficiency (*2,10*).

We adopted procedures for stable coupling of all 3 radiolabels to cetuximab without loss of immunoreactivity. The modification of the mAb and subsequent labeling of the mAb–chelate conjugate with ^{89}Zr has already been described in detail by Verel et al. (*18*). These procedures resulted in high labeling yields and specific activities. Coupling of DOTA and DTPA to mAbs and labeling with ^{88}Y or ^{177}Lu has been documented extensively. We standardized conjugation procedures to obtain a chelate-to-mAb molar ratio of 1:1, because higher ratios can dramatically alter the pharmacokinetics of the mAb (*23*).

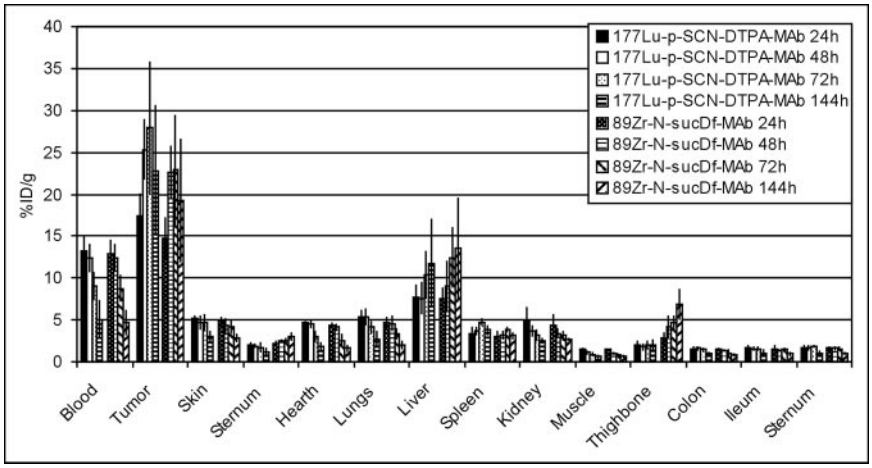

FIGURE 4. Biodistributions of intraperitoneally coinjected cetuximab-*N*-sucDf-^{89}Zr and cetuximab-*p*-SCN-Bz-DTPA-^{177}Lu (experiment 4, total of 500 μg mAb) in A431 xenograft-bearing nude mice at 24, 48, 72, and 144 h after injection.

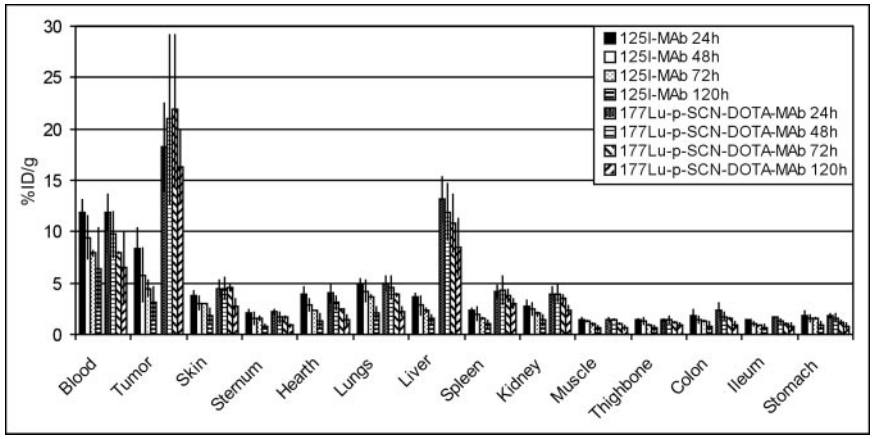

FIGURE 5. Biodistributions of intraperitoneally coinjected cetuximab-^{125}I and cetuximab-*p*-SCN-Bz-DOTA-^{177}Lu (experiment 5, total of 1 mg mAb) in A431 xenograft-bearing nude mice at 24, 48, 72, and 120 h after injection.

Preceding the biodistribution studies, the in vitro stability of the 5 radiometal conjugates in human serum was analyzed. The stability of all conjugates under these conditions was comparable and high until day 7. The ^{89}Zr-*N*-sucDf conjugate and the ^{88}Y/^{177}Lu-*p*-SCN-Bz-DOTA conjugates were especially stable during this period, showing less than 3% release. At later times, the ^{88}Y/^{177}Lu-*p*-SCN-Bz-DTPA conjugates and the ^{89}Zr-*N*-sucDf conjugate were less stable than the ^{88}Y/^{177}Lu-*p*-SCN-Bz-DOTA conjugates (at day 16, 22.4%/23.5% release for the ^{88}Y/^{177}Lu-*p*-SCN-Bz-DTPA conjugates and 17.4% for the ^{89}Zr-*N*-sucDf conjugate, vs. 4.0%/2.9% for the ^{88}Y/^{177}Lu-*p*-SCN-Bz-DOTA conjugates). Comparable differences in in vitro stability between ^{90}Y-DOTA-hLL2 and ^{90}Y-DTPA-hLL2 (0% vs. 3.6% dissociation after a 5-d incubation and 0.4% vs. 10.7% dissociation after an 11-d incubation) were previously reported by Govindan et al. (*22*). For ^{89}Zr-*N*-sucDf-mAb conjugates, stability data on later time points have been scarce thus far. Brouwers et al. (*24*) mentioned a less than 10% release of ^{89}Zr from cG250-*N*-sucDf during a 4-d incubation.

For easy comparison of the biodistributions, cetuximab-*N*-sucDf-^{89}Zr was administered to A431-bearing nude mice simultaneously with cetuximab-*p*-SCN-Bz-DOTA-^{88}Y, cetuximab-*p*-SCN-Bz-DOTA-^{177}Lu, cetuximab-*p*-SCN-Bz-DTPA-^{88}Y, or cetuximab-*p*-SCN-Bz-DTPA-^{177}Lu. Blood clearance was similar for all 5 conjugates. These results indicate that the pharmacokinetics of the mAb remained preserved on radiolabeling, irrespective of the type of chelate or radionuclide that had been used. Furthermore, the congruency of radioactivity levels in blood and several other organs in each individual mouse also indicated that the in vivo stability of the different chelate–radionuclide complexes was similar—results that agree with the in vitro serum stability measurements. Finally, tumor uptake levels indicate that the internalization rate of the radiolabeled conjugates and residualization of the 3 radiometals were similar within the period studied. Still, some differences in uptake between cetuximab-*N*-sucDf-^{89}Zr on the one hand and ^{88}Y- and ^{177}Lu-labeled cetuximab-*p*-SCN-Bz-DOTA/DTPA on the other hand were found in thighbone and, to a lesser degree, in sternum at all time points except 24 h after injection in thighbone for experiments 1 and 3. These data suggest that released ^{89}Zr or ^{89}Zr-containing metabolites might have a higher preference for thighbone and sternum than do the ^{88}Y and ^{177}Lu counterparts. Difference in bone accumulation has already been reported by Verel et al. (*14*). Between coinjected ^{89}Zr-labeled chimeric mAb U36 and ^{88}Y-labeled chimeric mAb U36, they found a difference of 2.5% ± 0.1 %ID/g versus 1.3% ± 0.1 %ID/g in thighbone at 72 h after injection and of 3.5% ± 0.4 %ID/g versus 1.1% ± 0.1 %ID/g at 144 h. The higher thighbone uptake of ^{89}Zr in our study might be related to the faster internalization rate of cetuximab than of chimeric mAb U36, which probably results in more extensive redistribution of bone-seeking ^{89}Zr-metabolites.

The bone marrow is generally the dose-limiting organ in nonmyeloablative RIT and is therefore important for dosimetric evaluations. For prediction of dose delivery to bone marrow in a combined immuno-PET/RIT setting, estimation of the bone marrow self-dose does not seem a problem, because blood levels were the same for the 3 radiometals. Dose delivery originating from radioactivity in the bone, however, will require an adjustment. Alternatively, differences in bone accumulation might be avoided by the development of a single chelate that binds ^{89}Zr, ^{88}Y, and ^{177}Lu with exactly the same high in vivo stability. The search for such an ideal chelate is part of our ongoing research. However, the use of the same chelate is not a guarantee for a congruent bone uptake. For example, differences in bone uptake have been observed between ^{111}In-mAb and ^{90}Y-mAb conjugates in vivo in tumor-bearing mice and in cancer patients, despite the fact that a single DTPA- or DOTA-like chelate was used for coupling of ^{111}In and ^{90}Y to the mAbs (*11,12*).

Intergroup differences make it difficult to draw firm conclusions about mutual differences in biodistribution between ^{88}Y and ^{177}Lu or between *p*-SCN-Bz-DOTA and *p*-SCN-Bz-DTPA conjugates. However, comparisons with the biodistribution of the ^{89}Zr-labeled-mAb that was coinjected as a reference conjugate in each case allow one to

conclude that the in vivo behaviors of ^{88}Y and ^{177}Lu are similar. This conclusion is in accordance with previous findings of Stein et al. (*25*). With respect to the *p*-SCN-Bz-DOTA versus the *p*-SCN-Bz-DTPA chelate, there is an indication of higher thighbone accumulation in the case of ^{88}Y/^{177}Lu-*p*-SCN-Bz-DTPA conjugates, an observation also described by others (*2,22,26*).

An alternative positron-emitting surrogate for estimation of the pharmacokinetics and biodistribution of ^{177}Lu/^{90}Y-labeled pharmaceuticals could be ^{86}Y (33% β^+; half-life, 14.7 h) (*12,27,28*). An advantage of ^{86}Y over ^{89}Zr is that the same chelate can be used for complexation of both ^{86}Y and ^{177}Lu/^{90}Y. Moreover, when ^{86}Y is used as a surrogate for ^{90}Y, decomplexation of the same element should result in identical tissue distribution, provided radioimmunoconjugate quality is identical. Unfortunately, ^{86}Y has 2 drawbacks: First, the half-life of ^{86}Y (14.7 h) might be ideal for imaging mAb fragments and peptides but is rather short for optimal imaging of intact mAbs. It takes typically 48–96 h for intact mAbs to achieve optimal tumor-to-nontumor ratios. This shorter half-life of ^{86}Y, compared with the half-life of ^{89}Zr (78.4 h), will also have disadvantages for logistics related to transportation and labeling of mAbs. Second, in contrast to ^{89}Zr, ^{86}Y emits prompt γ-photons, which together with 511-keV annihilation photons can result in so-called spurious true coincidences and therefore can introduce quantification artifacts (*29*). Solutions to these artifacts are under investigation (*30,31*).

CONCLUSION

In the present study, we showed that ^{89}Zr can perfectly predict the biodistribution of the residualizing labels ^{177}Lu and ^{88}Y in combination with the internalizing mAb cetuximab. The average uptake levels in tumor and other organs, except for thighbone and sternum, were similar for cetuximab-*N*-sucDf-^{89}Zr when compared with cetuximab-*p*-SCN-Bz-DOTA-^{88}Y, cetuximab-*p*-SCN-Bz-DOTA-^{177}Lu, cetuximab-*p*-SCN-Bz-DTPA-^{88}Y, and cetuximab-*p*-SCN-Bz-DTPA-^{177}Lu. In view of the advantages of PET over SPECT, ^{89}Zr-immuno-PET is a promising modality for in vivo scouting of ^{90}Y- and ^{177}Lu-labeled mAbs, although care should be taken when estimating bone marrow doses.

ACKNOWLEDGMENTS

This project was financially supported by STW (grant VBC.6120) and by the European Union FP6, LSHC-CT-2003–5032, STROMA. The content reflects only the authors' view. The European Commission is not liable for any use that may be made of the information. The authors thank BV Cyclotron for performing irradiations, Jan H. Rector (Solid State Physics, VU University) for sputtering ^{89}Y-copper supports, and Marianne Budde (VU University Medical Center) for contributing to the experiments.

REFERENCES

1. Sharkey RM, Goldenberg DM. Perspectives on cancer therapy with radiolabeled monoclonal antibodies. *J Nucl Med.* 2005;46(suppl):115S–127S.
2. Brouwers AH, Van Eerd JEM, Frielink C, et al. Optimization of radioimmunotherapy of renal cell carcinoma: labeling of monoclonal antibody cG250 with ^{131}I, ^{90}Y, ^{177}Lu, or ^{186}Re. *J Nucl Med.* 2004;45:327–337.
3. Press OW, Shan D, Howell-Clark J, et al. Comparative metabolism and retention of iodine-125, yttrium-90, and indium-111 radioimmunoconjugates by cancer cells. *Cancer Res.* 1996;56:2123–2129.
4. Sharkey RM, Behr TM, Mattes MJ, et al. Advantage of residualizing radiolabels for an internalizing antibody against the B-cell lymphoma antigen, CD22. *Cancer Immunol Immunother.* 1997;44:179–188.
5. Börjesson PKE, Postema EJ, de Bree R, et al. Radioimmunodetection and radioimmunotherapy of head and neck cancer. *Oral Oncol.* 2004;40:761–772.
6. de Jong M, Breeman WA, Valkema R, Bernard BF, Krenning EP. Combination radionuclide therapy using ^{177}Lu- and ^{90}Y-labeled somatostatin analogs. *J Nucl Med.* 2005;46(suppl):13S–17S.
7. Fink-Bennett DM, Thomas K. ^{90}Y-Ibritumomab tiuxetan in the treatment of relapsed or refractory B-cell non-Hodgkin's lymphoma. *J Nucl Med Technol.* 2003;31:61–68.
8. Seldin DW. Techniques for using Bexxar for the treatment of non-Hodgkin's lymphoma. *J Nucl Med Technol.* 2002;30:109–114.
9. Verel I, Visser GWM, van Dongen GA. The promise of immuno-PET in radioimmunotherapy. *J Nucl Med.* 2005;46(suppl):164S–171S.
10. Milenic DE, Garmestani K, Chappell LL, et al. In vivo comparison of macrocyclic and acyclic ligands for radiolabeling of monoclonal antibodies with ^{177}Lu for radioimmunotherapeutic applications. *Nucl Med Biol.* 2002;29:431–442.
11. Carrasquillo JA, White JD, Paik CH, et al. Similarities and differences in ^{111}In- and ^{90}Y-labeled 1B4M-DTPA antiTac monoclonal antibody distribution. *J Nucl Med.* 1999;40:268–276.
12. Camera L, Kinuya S, Garmestani K, et al. Comparative biodistribution of indium- and yttrium-labeled B3 monoclonal antibody conjugated to either 2-(p-SCN-Bz)-6-methyl-DTPA (1B4M-DTPA) or 2-(p-SCN-Bz)-1,4,7,10-tetraazacyclododecane tetraacetic acid (2B-DOTA). *Eur J Nucl Med.* 1994;21:640–646.
13. Garmestani K, Milenic DE, Plascjak PS, Brechbiel MW. A new and convenient method for purification of ^{86}Y using a Sr(II) selective resin and comparison of biodistribution of ^{86}Y and ^{111}In labeled Herceptin. *Nucl Med Biol.* 2002;29:599–606.
14. Verel I, Visser GWM, Boellaard R, et al. Quantitative ^{89}Zr immuno-PET for in vivo scouting of ^{90}Y-labeled monoclonal antibodies in xenograft-bearing nude mice. *J Nucl Med.* 2003;44:1663–1670.
15. Fan Z, Lu Y, Wu X, Mendelsohn J. Antibody-induced epidermal growth factor receptor dimerization mediates inhibition of autocrine proliferation of A431 squamous carcinoma cells. *J Biol Chem.* 1994;269:27595–27602.
16. Mendelsohn J, Baselga J. Status of epidermal growth factor receptor antagonists in the biology and treatment of cancer. *J Clin Oncol.* 2003;21:2787–2799.
17. Sunada H, Peacock J, Mendelsohn J. Ligand induced internalization of epidermal growth factor receptors by A431 cells decreases at high cell densities in culture. *Growth Factors.* 1991;5:45–55.
18. Verel I, Visser GWM, Boellaard R, Stigter-Van Walsum M, Snow GB, Van Dongen GAMS. ^{89}Zr Immuno-PET: comprehensive procedures for the production of ^{89}Zr-labeled monoclonal antibodies. *J Nucl Med.* 2003;44:1271–1281.
19. Visser GWM, Klok RP, Gebbinck JWK, Ter Linden T, Van Dongen GAMS, Molthoff CF. Optimal quality ^{131}I-monoclonal antibodies for high-dose labeling in a large reaction volume and temporarily coating the antibody with IODOGEN. *J Nucl Med.* 2001;42:509–519.
20. Lindmo T, Boven E, Cuttitta F, Fedorko J, Bunn PA. Determination of the immunoreactive fraction of radiolabeled monoclonal-antibodies by linear extrapolation to binding at infinite antigen excess. *J Immunol Methods.* 1984;72:77–89.
21. Meares CF, McCall MJ, Reardan DT, Goodwin DA, Diamanti CI, McTigue M. Conjugation of antibodies with bifunctional chelating agents: isothiocyanate and bromoacetamide reagents, methods of analysis, and subsequent addition of metal ions. *Anal Biochem.* 1984;142:68–78.
22. Govindan SV, Shih LB, Goldenberg DM, et al. ^{90}Yttrium-labeled complementarity-determining-region-grafted monoclonal antibodies for radioimmunotherapy: radiolabeling and animal biodistribution studies. *Bioconjug Chem.* 1998;9:773–782.
23. van Gog FB, Visser GW, Stroomer JW, Roos JC, Snow GB, Van Dongen GAMS.

High dose rhenium-186-labeling of monoclonal antibodies for clinical application: pitfalls and solutions. *Cancer.* 1997;80(suppl):2360S–2370S.
24. Brouwers A, Verel I, van Eerd J, et al. PET radioimmunoscintigraphy of renal cell cancer using ^{89}Zr-labeled cG250 monoclonal antibody in nude rats. *Cancer Biother Radiopharm.* 2004;19:155–163.
25. Stein R, Govindan SV, Chen S, et al. Radioimmunotherapy of a human lung cancer xenograft with monoclonal antibody RS7: evaluation of ^{177}Lu and comparison of its efficacy with that of ^{90}Y and residualizing ^{131}I. *J Nucl Med.* 2001;42:967–974.
26. Griffiths GL, Govindan SV, Sharkey RM, Fisher DR, Goldenberg DM. ^{90}Y-DOTA-hLL2: an agent for radioimmunotherapy of non-Hodgkin's lymphoma. *J Nucl Med.* 2003;44:77–84.
27. Pauwels S, Barone R, Walrand S, et al. Practical dosimetry of peptide receptor radionuclide therapy with ^{90}Y-labeled somatostatin analogs. *J Nucl Med.* 2005; 46(suppl):92S–98S.
28. Lovqvist A, Humm JL, Sheikh A, et al. PET imaging of ^{86}Y-labeled anti-Lewis Y monoclonal antibodies in a nude mouse model: comparison between ^{86}Y and ^{111}In radiolabels. *J Nucl Med.* 2001;42:1281–1287.
29. Pentlow KS, Finn RD, Larson SM, Erdi YE, Beattie BJ, Humm JL. Quantitative imaging of yttrium-86 with PET: the occurrence and correction of anomalous apparent activity in high density regions. *Clin Positron Imaging.* 2000;3:85–90.
30. Buchholz HG, Herzog H, Forster GJ, et al. PET imaging with yttrium-86: comparison of phantom measurements acquired with different PET scanners before and after applying background subtraction. *Eur J Nucl Med Mol Imaging.* 2003;30:716–720.
31. Walrand S, Jamar F, Mathieu I, et al. Quantitation in PET using isotopes emitting prompt single gammas: application to yttrium-86. *Eur J Nucl Med Mol Imaging.* 2003;30:354–361.